

# Design and simulation of rotated hexagonal porous core photonic crystal fibre with improved effective material loss and dispersion properties

Izaddeen Kabir Yakasai, Pg. Emeroylariffion Abas, Norazanita Hj Shamsuddin, Feroza Begum  
Department of Systems Engineering, Faculty of Integrated Technologies,  
Universiti Brunei Darussalam, Brunei Darussalam

---

## Article Info

### Article history:

Received Feb 1, 2020

Revised Apr 4, 2020

Accepted Apr 18, 2020

---

### Keywords:

Dispersion  
Effective material loss  
Photonic crystal fibre  
Single-mode fibre  
Terahertz

---

## ABSTRACT

A thorough modal characterization, centred on the full vectorial finite element method (FEM) has been used to model and numerically investigate a porous core photonic crystal fibre (PC-PCF), which may potentially be integrated into Terahertz (1012Hz) compact systems. The proposed fibre consists of a rotated hexagonal core surrounded by a conventional hexagonal cladding. It has been shown that effective material loss (EML), core power fraction and dispersion profile are  $0.019\text{cm}^{-1}$ , 51.7% and  $0.5 \pm 0.04\text{ps/THz/cm}$  within 1THz bandwidth, respectively. Based on simulated results and noncomplex design, it is envisaged that the proposed fibre can be realised for industrial THz applications

Copyright © 2020 Institute of Advanced Engineering and Science.  
All rights reserved.

---

### Corresponding Author:

Izaddeen Kabir Yakasai,  
Department of Systems Engineering,  
Faculty of Integrated Technologies,  
Universiti Brunei Darussalam, Jalan Tungku Link, BE1410, Brunei Darussalam.  
Email: 17h0892@ubd.edu.bn, muhddeen1@gmail.com

---

## 1. INTRODUCTION

Development of THz waveguides has rapidly progressed in the last two decades [1]. Waveguide solutions used in the early days include metallic wires, dielectric tubes with metallic coatings, sub-wavelength dielectric fibres, hollow-core polymer fibres and solid-core photonic crystal fibres (SC-PCFs) [2]. However, these solutions have been proven to be inadequate due to high-frequency dependent attenuation and dispersion, among other factors. SC-PCF consists of solid dielectric in the core region and an array of air holes serving as low index discontinuities in the cladding region. Even though light guidance in SC-PCFs follows modified total internal reflection (MTIR) mechanism, the lights are impaired with high-frequency dependent attenuation and dispersion [3, 4]. Further air hole discontinuities may be introduced in the core region to reduce attenuation and dispersion, to form what is now popularly known as porous core photonic crystal fibre (PC-PCF) [2]. Common polymers used as background materials for PC-PCFs include Zeonex, Teflon, poly-methyl methacrylate (PMMA) and cyclic olefin co-polymer; with cyclic olefin co-polymer, commercially known as TOPAS, being the most optically transparent polymer within 0.2-2THz frequency range and hence, commonly used. Some properties of TOPAS include flat refractive index of 1.5258 within 0.2-2THz frequency range [5], low bulk material absorption loss of  $0.2\text{cm}^{-1}$ , negligible absorption of moisture and bio-sensing capabilities [6, 7]. Propagated THz waves in PC-PCFs face the risk of being absorbed by the background material and may scatter across various fibre regions. Another issue faced by PC-PCFs is chromatic dispersion. Designing PC-PCFs to address these issues is challenging and requires geometrical parameters to be optimized based on their position, shape and size.

Previously reported rotated hexagonal core PC-PCFs in [8, 9] have exhibited EMLs of  $0.066\text{cm}^{-1}$  and  $0.045\text{cm}^{-1}$ , and core power fraction of 40% and 31.25%, respectively. Dispersion variations for both fibres are reported to be above  $\pm 0.06\text{ps/THz/cm}$ . Generally, low EML and dispersion variation improve light guidance as well as the information-carrying capacity of the fibre. Improved power fraction of 45% has been achieved using circular core lattice in [10], although EML ( $\alpha_{\text{eff}}=0.063\text{cm}^{-1}$ ) and dispersion variation ( $0.55\text{ps/THz/cm}$ ) are comparatively higher. Some other PC-PCFs designs have also been reported [11-13], however, high EMLs and dispersion variation, and comparatively low core power fractions, have been obtained as compared to EMLs, dispersion and core power fraction of proposed PC-PCF in this paper. Other than these parameters, it is also important to determine bending loss of PC-PCF at different bend radii as high bending loss may affect flexibility of the fibre in applications such as THz endoscopy, which necessitates bending.

## 2. GEOMETRY OF THE PROPOSED DESIGN

Cross-section of the proposed PC-PCF is shown in Figure 1. Its core follows a rotated hexagonal lattice structure at 90 degrees with the distance between centres of two adjacent air holes or its pitch denoted by  $\Lambda_c$ . Porosity, which is the ratio of the total area of all core air holes to the cross-sectional area of the core, determines core air hole size  $d_c$  and consequently, core air filling fraction  $F_c=d_c/\Lambda_c$ . The core has diameter  $D_{\text{core}}=2(\Lambda-d/2)$ , where  $\Lambda$  and  $d$ , are cladding pitch and cladding air hole diameter, respectively. Cladding air filling fraction  $F_{cl}$  is kept at high value to make the core optically denser than the cladding so that MTIR mechanism can be preserved [14]. Similar to its core, air holes in the cladding follow five (5) layers of hexagonal structure but with the innermost air hole substituted with the core. There are a total of 90 air holes in the cladding. A PML with a thickness of 8% of the total fibre radius is introduced to prevent the back-reflection of light onto the fibre.

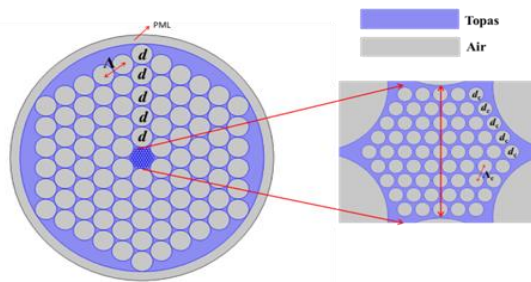


Figure 1. Cross-section of the proposed hexagonal cladding with an enlarged image of the rotated hexagonal core

## 3. ANALYSIS METHOD

Design and simulation of the proposed PC-PCF have been carried out using Finite Element Method based COMSOL Multiphysics software V 5.3a. Finer element size meshing has been used so that all air holes can be correctly mapped. The complete mesh consists of 84,274 triangular elements, 8,095 edge elements and 612 vertex elements. Minimum and average element qualities have been observed to be 0.4268 and 0.9329 respectively, giving a very low computational error during the simulation. Perfectly matched layer (PML), which takes 8% of the total radius of the whole fibre, has been imposed outside the computational domain, to absorb incident radiation as well as prevent reflection of light back into the cladding area.

## 4. SIMULATION RESULTS

The electric field distribution of the proposed PC-PCF for 50%, 60%, 70%, 80% and 85% porosity at 1 THz frequency is provided in Figure 2 with red arrows indicating directions of propagation. The figure shows gradual delocalisation of light as porosity is increased, thus the need for an optimised parameter set. Confinement loss is a measurement on the amount of light loss from the core region and it strongly relies on the core-cladding refractive index contrast. Confinement loss  $L_c$  can be calculated by using the following expression [11, 15]:

$$L_c = 8.686 \left( \frac{2\pi f}{c} \right) \text{Im}(n_{\text{eff}}) \text{cm}^{-1} \quad (1)$$

where  $f$  is the operating frequency,  $c$  is the speed of light in free space, and  $\text{Im}(n_{\text{eff}})$  is the imaginary part of the effective refractive index of the fundamental mode.

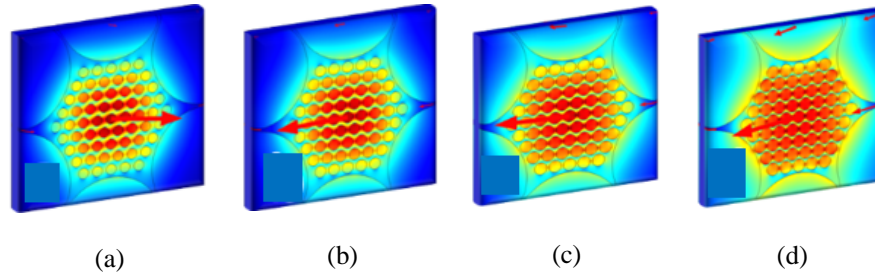


Figure 2. Electric field distribution of proposed PC-PCF at 1 THz and 320 μm Dcore for (a) 60%, (b) 70%, (c) 80% and (d) 85% porosities

EML in PC-PCFs emanates from the intrinsic loss of atoms in the material’s molecular structure due to heat resulting from its interaction with energy [16], and this translates into the absorption of THz waves. EML,  $\alpha_{\text{eff}}$  is calculated by using the following expression [17, 18];

$$\alpha_{\text{eff}} = \sqrt{\frac{\epsilon_0}{\mu_0} \left( \frac{\int_{\text{mat}} n_{\text{mat}} |E|^2 \alpha_{\text{mat}} dA}{2 \int_{\text{all}} S_z dA} \right)} \text{ cm}^{-1} \tag{2}$$

where  $\alpha_{\text{eff}}$  is the effective material loss  $\epsilon_0$  and  $\mu_0$  denote permittivity and permeability of free space, respectively,  $n_{\text{mat}}$  is the refractive index of Topas,  $E$  and  $\alpha_{\text{mat}}$  are modal electric field and bulk Topas absorption loss respectively whilst  $S_z$  is z-component of the Poynting vector.

Figure 3 shows the dependence of  $L_c$  and EML on core porosity. It can be seen that  $L_c$  increases whilst EML decrease with an increase in core porosity. Increasing porosity requires enlarging of core air holes thereby replacing bulk material present in the core with low index dry air. As a result, core-cladding index contrast becomes smaller and MTIR guidance weakens, leading to delocalisation of light from the core. EML reduces with an increase in porosity values due to a reduction in the amount of TOPAS in the core as porosity is increased. At 50% porosity and  $D_{\text{core}}=360\mu\text{m}$ ,  $L_c$  is lowest at  $3.74 \times 10^{-13} \text{cm}^{-1}$  with EML at its highest at  $0.044 \text{cm}^{-1}$ , whilst the converse is observed at 85% porosity and  $D_{\text{core}}=280\mu\text{m}$  where  $L_c=0.062 \text{cm}^{-1}$  and  $\alpha_{\text{eff}}=0.015 \text{cm}^{-1}$ . Therefore, 80% porosity and  $D_{\text{core}}=320\mu\text{m}$  have been selected as optimum values to serve as a trade-off between high confinement loss and low EML, and vice versa.

Relationship between  $L_c$  and EML with frequency is presented in Figure 4, where it can be seen that whilst  $L_c$  reduces with increase in frequency, EML increases. Both trends are due to the strong light-matter interaction as frequency increases, in other words, the higher the frequency, the higher the interaction between TOPAS and THz waves. Increased frequency broadens core-cladding index contrast and strengthens MTIR guidance. Consequently, this improves the convergence of fundamental mode field to the core region and reduces  $L_c$ . EML’s response to frequency is slower, slow and fast within 0.4-0.6THz, 0.6-1.6THz and 1.6-1.8THz ranges respectively, as can be seen in Figure 4. Light-matter interactions at respective frequency ranges correlate with the rate of material absorption, i.e. the higher the frequency, the faster TOPAS gets heated, losses molecules and absorb THz waves. At 1 THz operating frequency and selected porosity and  $D_{\text{core}}$  values,  $L_c$  and EML of the proposed PC-PCF are  $2.02 \times 10^{-3} \text{cm}^{-1}$  and  $0.019 \text{cm}^{-1}$ , respectively.

Since the material with the least opacity in THz frequencies is dry air, the geometry of the proposed fibre is designed such that majority of propagated power would transmit through the dry air holes in the core whilst at the same time preserving MTIR guidance. Power fraction,  $\eta'$  gives insight into propagated power concentration across various regions of the fibre, which is helpful for designing PC-PCFs, and it can be expressed as [19, 20]:

$$\eta' = \frac{\int_x S_z dA}{\int_{\text{all}} S_z dA} \times 100 \% \tag{3}$$

where  $x$  denotes the fibre region of interest. Besides the core air hole, power fractions in the cladding air holes and Topas material are also presented for convenience.

Relationship between power fraction and frequency is shown in Figure 5. At 1THz, it is shown that majority of the mode power is localised at the core air holes and core material; 51.7% propagating inside the core air holes and 21.4% propagating inside the core material with EML of  $0.019 \text{cm}^{-1}$ , with only 26.7% propagating outside of the core.

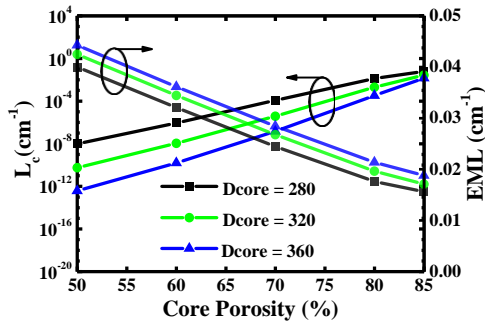


Figure 3. Confinement loss and EML of the proposed PC-PCF in relation to core porosity

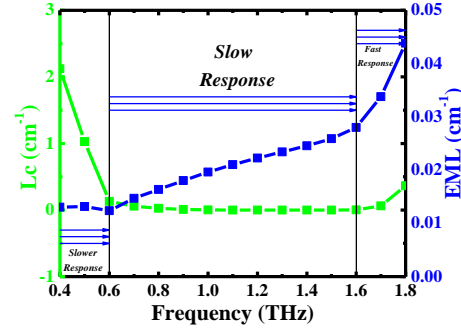


Figure 4. Relationship between Lc and EML with operating frequency

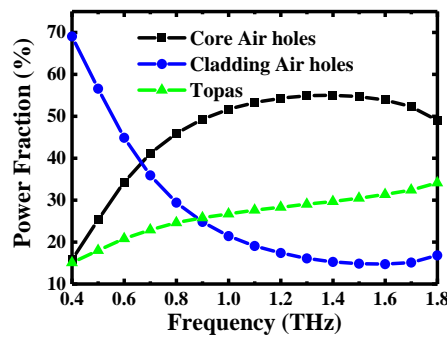


Figure 5. Power fraction of the proposed PC-PCF for core air holes, cladding air holes and core material region

Applications such as in-vivo THz imaging may require the fibre to deliver a large beam of THz light. Effective area  $A_{eff}$  is a quantification of the area covered by the fundamental mode and it can be expressed by using the following [6, 21]:

$$A_{eff} = \frac{[\int I(r)rdr]^2}{\int I^2(r)rdr} \mu m^2 \tag{4}$$

where  $I(r)$  refers to the intensity of light.

Some THz applications may also require the fibre to be bent to a certain curvature. The flexibility of the proposed fibre can be ascertained by measuring the loss it incurs during bending. Bend loss can be approximated using the following analytical expression [22, 23]:

$$\alpha_{BL} = \frac{1}{8} \sqrt{\frac{2\pi}{3}} \frac{1}{A_{eff}} \frac{1}{\beta} F \left[ \frac{2}{3} R \frac{((\beta^2 - \beta_{cl}^2)^{\frac{3}{2}})}{\beta^2} \right] cm^{-1} \tag{5}$$

where  $F(x) = x^{-\frac{1}{2}} e^{-x}$ ,  $\beta = \frac{2\pi n_{co}}{\lambda}$  and  $\beta_{cl} = \frac{2\pi n_{cl}}{\lambda}$  are propagation constants of the core and cladding, respectively.  $n_{co}$  and  $n_{cl}$  are refractive indexes of the core and cladding.  $n_{cl}$  can be calculated using the following [24]:

$$n_{cl} = \sqrt{F_{cl} + (1 - F_{cl})n_s} \tag{6}$$

where  $F_{cl}$  is the cladding refractive index and  $n_s$  is TOPAS refractive index.

From Figure 6, it can be deduced that effective area is sufficiently large,  $A_{eff} = 3.4 \times 10^5 \mu m^2$  and bend loss is very small  $\alpha_{BL} = 5.79 \times 10^{-6} cm^{-1}$  at 1 THz operating frequency. Bend loss is calculated for a minimum bend radius of 1cm as reducing its radius further may require the use of excessive force or heat. V-parameter is used to determine the region of single-mode operation in PC-PCFs and is calculated using [11]:

$$V = \frac{2\pi r f}{c} \sqrt{n_{co}^2 - n_{cl}^2} \leq 2.405 \tag{7}$$

where  $r, f,$  and  $c$  are core radius, frequency and velocity of light in free space. The fibre becomes multi-mode if V-parameter value is 2.405 above.

It is shown in Figure 7 that the proposed fibre operates as a single-mode fibre within a wide frequency range of between 0.4-1.5THz i.e. 1.1THz band. The single mode region is not analysed below 0.4THz because the fibre produces high scattering which leads to high losses at lower frequencies, i.e. 0.1-0.39THz. Chromatic dispersion provides information on pulse broadening that occurs as a result of optical sub-pulses traversing the fibre with different propagation constants. Although chromatic dispersion is a combination of material and waveguide dispersions, material dispersion is discarded for the proposed fibre as TOPAS has negligible material dispersion in THz frequencies. Waveguide dispersion or group velocity dispersion, measured in ps/THz/cm, can be calculated using the following expression [25];

$$\beta_2 = \frac{2}{c} \frac{dn_{eff}}{d\omega} + \frac{\omega}{c} \frac{d^2n_{eff}}{d\omega^2} \text{ ps/THz/cm} \tag{8}$$

where  $n_{eff}$  denotes the effective refractive index,  $\omega$  is angular centre frequency and  $c$  is the velocity of light in free space. Near zero ultra-flattened dispersion allows THz sub-pulses to be transmitted simultaneously with nearly equal pulse spreading.

From Figure 8, it can be seen that the proposed fibre demonstrates near-zero ultra-flattened dispersion profile  $0.5 \pm 0.04$ ps/THz/cm within 0.5-1.5THz range (1THz band). The obtained flattened dispersion points to the suitability of the proposed fibre for multichannel THz communication applications. A comparison of the proposed rotated hexagonal PC-PCF and previously published PC-PCFs, is presented in Table 1. The proposed fibre exhibits EML value that much lower than proposed PC-PCFs as shown in Table 1. Although a low EML of 0.016 cm<sup>-1</sup> has been obtained in [11], bending loss has not been ascertained. Table 1 also shows that the power fraction and dispersion profile of the proposed fibre are superior to recently published works.

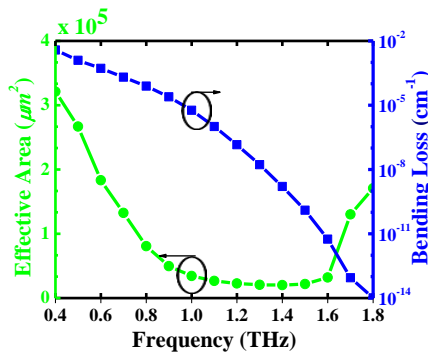


Figure 6. Effective area and bending loss of the proposed PC-PCF for in relation to frequency

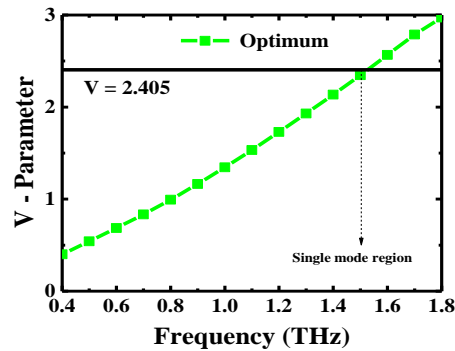


Figure 7. V-parameter of the proposed fibre in relation to frequency

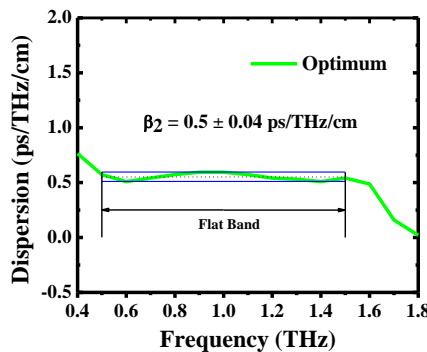


Figure 8. Dispersion profile of the proposed fibre showing flattened dispersion region

Table 1. Comparison with previously reported PC-PCFs

Ref	Structure	$\alpha_{\text{eff}}$ (cm <sup>-1</sup> )	$\eta'$ (%)	$\beta_2$ (ps/THz/cm)	$\alpha_{\text{BL}}$ (cm <sup>-1</sup> )
[8]	Hex-Hex	0.066	40	$\pm 0.12$	10 <sup>-1</sup>
[9]	Hex-Hex	0.04	31.3	$\pm 0.07$	-
[10]	Hexa-Cir	0.06	45	$\pm 0.55$	10 <sup>-11</sup>
[11]	Star	0.01	50	$\pm 10$	-
[12]	Cir-Hyb	0.04	26.8	-	-
[13]	Cir-Ellp	0.07	38	$\pm 0.32$	10 <sup>-13</sup>
Proposed PC-PCF	Hex-Hex	0.01	51.7	$\pm 0.04$	10 <sup>-6</sup>

## 5. CONCLUSION

A PC-PCF with conventional hexagonal cladding and rotated hexagonal core has been reported in this paper. It has been shown that with a core diameter of 320 $\mu\text{m}$ , an EML of 0.019cm<sup>-1</sup> and core power fraction of 51.7% can be achieved. The fibre's dispersion profile is 0.5  $\pm$  0.07ps/THz/cm within 1.4 THz bandwidth. Bending loss of the proposed fibre has been found to be negligibly low 5.78 $\times$ 10<sup>-6</sup> cm<sup>-1</sup> for 1cm bend radius. An integral improvement provided in this design is the calculation of exact cladding refractive index when calculating V-parameter. It has also been shown that the proposed PC-PCF operates as a single-mode fibre for a wide range of frequencies. It is anticipated that the design may be fabricated and integrated into compact THz applications as a flexible waveguide.

## REFERENCES

- [1] H. A. Abdalnabi, M. A. Shuriji, and S. Ahmed, "UWB THz plasmonic microstrip antenna based on graphene," *TELKOMNIKA (Telecommunication, Computing, Electronics and Control)*, vol. 18, no. 1, pp. 30-36, 2020.
- [2] I. K. Yakasai, P. E. Abas, H. Suhaimi, and F. Begum, "Low loss and highly birefringent photonic crystal fibre for terahertz applications," *Optik*, vol. 206, p. 164321, 2020.
- [3] S. Atakaramians, S. Afshar, T. M. Monro, and D. Abbott, "Terahertz dielectric waveguides," *Advances in Optics and Photonics*, vol. 5, no. 2, pp. 169-215, 2013.
- [4] Y. Yang, "Atmospheric Effects on Free-Space THz THz Time-Domain Spectroscopy (THz-TDS)," *Journal of Lasers, Optics & Photonics*, vol. 1, no. 2, pp. 1-2, 2014.
- [5] G. Khanarian and H. Celanese, "Optical properties of cyclic olefin copolymers," *Journal of Optical Microsystems*, vol. 40, no. 6, pp. 1024-1030, 2001.
- [6] I. K. Yakasai, P. E. Abas, S. Ali, and F. Begum, "Modelling and simulation of a porous core photonic crystal fibre for terahertz wave propagation," *Optical and Quantum Electronics*, vol. 51, no. 122, pp. 1-16, 2019.
- [7] Darwison et al., "A leakage current estimation based on thermal image of polymer insulator," *Indonesian Journal of Electrical Engineering and Computer Science*, vol. 16, no. 3, pp. 1096-1106, 2019.
- [8] R. Islam, G. K. M. Hasanuzzaman, M. S. Habib, S. Rana, and M. A. G. Khan, "Low-loss rotated porous core hexagonal single-mode fiber in THz regime," *Optical Fiber Technology*, vol. 24, pp. 38-43, 2015.
- [9] R. Islam, G. K. M. Hasanuzzaman, M. A. Sadath, S. Rana, and M. S. Habib, "Extremely low-loss single-mode photonic crystal fiber in the terahertz regime," *2015 International Conference on Electrical & Electronic Engineering (ICEEE)*, Rajshahi, pp. 289-292, 2015.
- [10] M. A. Habib and M. S. Anower, "A novel low loss porous-core photonic crystal fiber for terahertz wave transmission," *2017 International Conference on Electrical, Computer and Communication Engineering (ECCE)*, Cox's Bazar, pp. 56-59, 2017.
- [11] F. Ahmed, S. Roy, K. Ahmed, B. K. Paul, and A. N. Bahar, "A novel star shape photonic crystal fiber for low loss terahertz pulse propagation," *Nano Communication Networks*, vol. 19, pp. 26-32, 2019.
- [12] K. M. S. Reza, B. K. Paul, and K. Ahmed, "Highly birefringent, low loss single-mode porous fiber for THz wave guidance," *Results in Physics*, vol. 11, pp. 549-553, 2018.
- [13] M. A. Habib and M. S. Anower, "Design and numerical analysis of highly birefringent single mode fiber in THz regime," *Optical Fiber Technology*, vol. 47, pp. 197-203, 2019.
- [14] M. N. Petrovich et al., "Microstructured fibers for sensing applications," *Journal of Optical Microsystems*, vol. 6005, 2005.
- [15] F. Begum and Y. Namihir, "Photonic Crystal Fiber for Medical Applications," in *Recent Progress in Optical Fiber Research*, pp. 229-246, 2012.
- [16] A. A. Binti Anis, C. B. M. Bin Rashidi, and S. A. Aljunid, "Analysis using multiple free space optic channel with amplification to mitigate haze attenuation," *Indonesian Journal of Electrical Engineering and Computer Science*, vol. 14, no. 2, pp. 546-554, 2019.
- [17] A. Hassani, A. Dupuis, and M. Skorobogatiy, "Low loss porous terahertz fibers containing multiple subwavelength holes," *Applied Physics Letters*, vol. 92, no. 7, p. 071101, 2008.
- [18] M. R. Islah, M. F. Kabir, K. M. A. Talha, and M. S. Islam, "A novel hollow core terahertz refractometric sensor," *Sensing and Bio-Sensing Research*, vol. 25, p. 100295, Sep. 2019.
- [19] I. Yakasai, P. E. Abas, S. Kaijage, and F. Begum, "Novel HRS-based porous core photonic crystal fibre for terahertz wave guidance," *International Journal of Electrical and Electronic Engineering & Telecommunications*, vol. 9, no. 1, pp. 62-67, 2020.

- [20] B. Paul et al., "A Novel Hexahedron Photonic Crystal Fiber in Terahertz Propagation: Design and Analysis," *Photonics*, vol. 6, no. 1, pp. 32-39, 2019.
- [21] F. Begum, Y. Namihira, T. Kinjo, and S. Kaijage, "Supercontinuum generation in photonic crystal fibres at 1.06, 1.31, and 1.55m wavelengths," *Electronics Letters*, vol. 46, no. 22, pp. 1518-1520, 2010.
- [22] S. F. Kaijage, Z. Ouyang, and X. Jin, "Porous-core photonic crystal fiber for low loss terahertz wave guiding," *IEEE Photonics Technology Letters*, vol. 25, no. 15, pp. 1454-1457, 2013.
- [23] I. K. Yakasai, A. Rahman, P. E. Abas, and F. Begum, "Theoretical Assessment of a Porous Core Photonic Crystal Fiber for Terahertz Wave Propagation," *Journal of Optics/ Communications*, pp. 1-11, 2018.
- [24] T. A. Birks, J. C. Knight, and P. S. J. Russell, "Endlessly single-mode photonic crystal fiber," *Optics Letters*, vol. 22, no. 13, pp. 961-963, 1997.
- [25] I. Yakasai et al., "Proposal for a Quad-Elliptical Photonic Crystal Fiber for Terahertz Wave Guidance and Sensing Chemical Warfare Liquids," *Photonics*, vol. 6, no. 3, pp. 78-94, 2019.

## BIOGRAPHIES OF AUTHORS



**Izaddeen Yakasai** is a PhD student at the Faculty of Integrated Technologies, Universiti Brunei Darussalam in Brunei Darussalam. His current research interests include nonlinear optics, optoelectronics, design and optimization of photonic crystal fibres, photonic sensors, especially in the terahertz regime.



**Pg E. Abas** is an assistant professor in System Engineering, Faculty of Integrated Technologies, Universiti Brunei Darussalam. His present research interests are data analysis, security of information communication systems and design of photonic crystal fibre in fibre optics communication.



**Norazanita Shamsudin** is a Lecturer of Chemical and Process Engineering, Faculty of Integrated Technologies, Universiti Brunei Darussalam. Her present research interests are water pollution and wastewater management, membrane technologies, PoUWT systems, environmental analysis/monitoring, etc.



**Feroza Begum** is an assistant professor in System Engineering at Faculty of Integrated Technologies, Universiti Brunei Darussalam (UBD) in Brunei Darussalam. She is engaged in research on optical fibre and photonics, photonic crystal fibres, optical fibre communications, optical coherence tomography, terahertz wave technology and optical sensors.